Acta Crystallographica Section F
Structural Biology and Crystallization Communications
ISSN 1744-3091

Structure of *Citrobacter freundii* L-methionine γ-lyase

D. V. Mamaeva,[a] E. A. Morozova,[a] A. D. Nikulin,[b] S. V. Revtovich,[a] S. V. Nikonov,[b] M. B. Garber[b] and T. V. Demidkina[a]*

[a]Engelhardt Institute of Molecular Biology, Russian Academy of Sciences, Vavilov str. 32, 119991 Moscow, Russia, and [b]Institute of Protein Research, Russian Academy of Sciences, 142290 Pushchino, Moscow Region, Russia

Correspondence e-mail: tvd@eimb.ru

Received 22 March 2005
Accepted 14 May 2005
Online 1 June 2005

PDB Reference: L-methionine γ-lyase, 1y4i, r1y4isf.

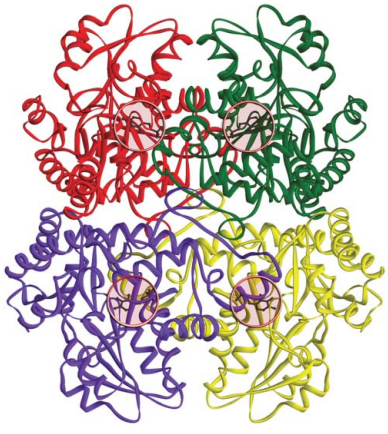

L-Methionine γ-lyase (MGL) is a pyridoxal 5′-phosphate (PLP) dependent enzyme that catalyzes γ-elimination of L-methionine. The crystal structure of MGL from *Citrobacter freundii* has been determined at 1.9 Å resolution. The spatial fold of the protein is similar to those of MGLs from *Pseudomonas putida* and *Trichomonas vaginalis*. The comparison of these structures revealed that there are differences in PLP-binding residues and positioning of the surrounding flexible loops.

1. Introduction

L-Methionine γ-lyase (MGL; EC 4.4.1.11) catalyzes PLP-dependent γ-elimination and γ-replacement reactions of L-methionine and its derivatives as well as β-elimination and β-replacement reactions of L-cysteine and S-substituted L-cysteines (Tanaka *et al.*, 1977, 1985). MGL has been isolated from a number of bacteria, including *Pseudomonas putida*, *Aeromonas* sp., *Clostridium sporogenes*, *P. taetrolens* and *Brevibacterium linens*, and from the primitive protozoa *Entamoeba hystolytica* and *Trichomonas vaginalis*. There has been increasing interest in this enzyme as methionine-dependency has been reported in cancer cell lines and primary tumours. The enzyme has been found to be an effective anti-tumour agent *in vitro* and *in vivo* and to be of potential value in the treatment of Parkinson's disease, arteriosclerosis, aging and obesity (Hoffman, 1997). Sulfur amino-acid metabolism in bacteria is not yet fully understood and it is likely that many bacteria possess MGL. Thus, inhibitors of this enzyme could ultimately prove to be effective against pathogens. Moreover, since mammals apparently do not possess MGL, the enzyme is a promising target for anti-trichomonad and anti-entamoeba chemotherapy.

Despite the potential importance of MGL in medicine, the mechanism of the enzyme has not been well studied. Recently, crystal structures of MGL from *P. putida* (Motoshima *et al.*, 2000; PDB codes 1gc0, 1ukj and 1pg8) and from *T. vaginalis* (PDB codes 1e5f and 1e5e) have been determined. This opens a route for study of the structure–functional basis of the catalysis of the γ- and β-elimination reactions that are catalyzed by MGL.

It has been shown that *Citrobacter intermedius* cells produce MGL when grown on a medium containing lactate and L-methionine (Faleev *et al.*, 1994). We have cloned and sequenced the gene of *C. freundii* MGL and overexpressed the protein in *Escherichia coli* BL21 (DE3) cells containing the plasmid pET-15b (Manukhov *et al.*, 2005). A comparison of the kinetic parameters of MGLs from *C. freundii*, *P. putida* and *T. vaginalis* showed that the K_m values of these enzymes were relatively similar, while significant variations in reaction rates were observed (Demidkina *et al.*, unpublished work). To explain the observed differences in the kinetic behaviour of enzymes from different species, further mechanistic and structural studies must be undertaken. In this paper, we report details of the crystallization of *C. freundii* MGL and the three-dimensional structure of the holoenzyme at 1.9 Å resolution.

2. Materials and methods

2.1. Crystallization

Crystals of MGL were obtained using the hanging-drop vapour-diffusion technique at 303 K. All drops were generated by mixing 2.0 µl of the enzyme dialyzed into 50 m*M* Tris–HCl pH 8.5, 0.5 m*M* PLP, 0.2 m*M* DTT with 2.0 µl of a precipitant solution on siliconized cover slides and were equilibrated against 1.0 ml of the same precipitant solution. MGL formed crystals with two precipitant solutions: (i) 35–37% polyethylene glycol monomethyl ether (PEG MME) 2000, 200 m*M* ammonium sulfate, 50 m*M* Tris–HCl pH 8.5, 0.2 m*M* PLP, 25 m*M* DTT and (ii) the same solution without ammonium sulfate. Rhombic shaped crystals appeared after a week and attained dimensions of 0.3 mm within two weeks. Crystals obtained using solution (i) were used to collect a data set. These crystals belong to space group *I*222, with unit-cell parameters a = 56.35, b = 121.83, c = 127.16 Å, and contain one subunit in the asymmetric unit. Prior to freezing in liquid nitrogen, the crystals were transferred to 37% PEG MME 2000, 200 m*M* ammonium sulfate, 50 m*M* Tris–HCl pH 8.5, 0.2 m*M* PLP, 25 m*M* DTT. Data from a single crystal were collected on the EMBL PX beamline BW7A at the DORIS storage ring, DESY (Hamburg, Germany) using a MAR CCD detector and were processed using the *XDS* program (Kabsch, 1993). Detailed data-collection statistics are shown in Table 1.

2.2. Structure determination and refinement

The *AMoRe* program package (Navaza, 1994) was used to solve the structures by the molecular-replacement method. A monomer of MGL from *P. putida* (PDB code 1gc0) with appropriate changes in the sequence was used as a model. For diffraction data between 15 and 3.0 Å, the model gave clear solutions with a correlation coefficient of 44.8 and an R factor of 59.8%. The structure was further subjected to several rounds of computational refinement and map calculation with *CNS* (Brünger *et al.*, 1998) and manual model inspection and modification with *O* (Jones *et al.*, 1991). A free R factor calculated from 5% of reflections set aside at the outset was used to monitor the progress of refinement. The initial anisotropic overall B factor was replaced successively with per-residue B factors, separate per-residue B factors for main- and side-chain atoms and, finally, restrained individual atomic B factors. The model bias present in the initial molecular-replacement solutions was tackled using composite omit cross-validated σ_A-weighted maps implemented in *CNS*. The electron-density map was of sufficient quality (Fig. 1) to trace whole polypeptide chains, including residues 2–398.

When the R-factor value reached 30%, water molecules were placed into 3σ peaks in $F_o - F_c$ maps when they were within suitable hydrogen-bonding distance of the existing model. After refinement, water molecules whose positions were not supported by the electron density at 1σ contouring in a σ_A-weighted $2F_o - F_c$ map were deleted. The final model refined to 1.9 Å incorporates 3024 non-H atoms (Table 1) and was deposited in the PDB (code 1y4i).

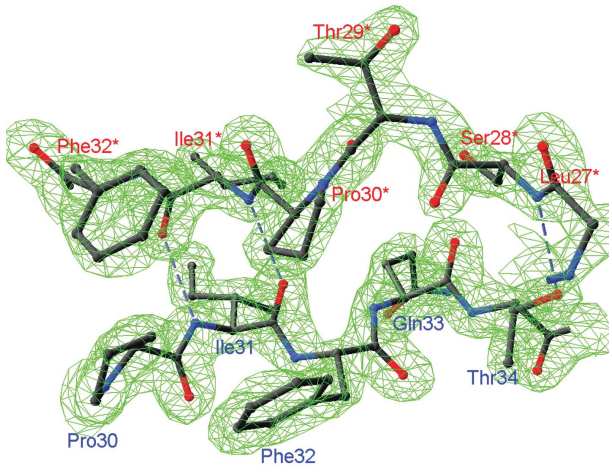

Figure 1
A fragment of the final $2F_o - F_c$ map contoured at the 2.0σ level in the region of the short antiparallel β-sheet connecting two MGL monomers.

Table 1
Data-collection and refinement statistics.

Values in parentheses are for the highest resolution shell.

Space group	*I*222
Unit-cell parameters (Å)	a = 56.35, b = 121.83, c = 127.16
Wavelength (Å)	0.843
Resolution (Å)	20–1.9 (2.0–1.9)
Completeness (%)	95.2 (83.9)
$I/\sigma(I)$	18.3 (4.1)
Redundancy	4.0 (3.7)
R_{merge} (%)	5.7 (38.2)
No. non-H protein atoms	3024
No. solvent atoms	104
Resolution range (Å)	20–1.9
No. reflections	33874
R (%)	20.6
R_{free} (%)	20.9
Mean temperature factor B (Å^2)	32.4
R.m.s. deviation from ideal values	
Bond lengths (Å)	0.022
Bond angles (°)	1.6
Dihedral angles (°)	24.1
Improper angles (°)	2.08
Ramachandran plot	
Most favoured	303 [87.8%]
Additionally allowed	37 [11.0%]
Generously allowed	4 [1.2%]

3. Results and discussion

MGL belongs to the evolutionary γ-family of PLP-dependent enzymes (Alexander *et al.*, 1994) involved in the metabolism of sulfur-containing amino acids. The three-dimensional structures of PLP-dependent enzymes belong to five distinct folds: types I–V (John, 1995; Jansonius, 1998; Alexander *et al.*, 1994; Grishin *et al.*, 1995; Qu *et al.*, 1998). Aspartate aminotransferase (AAT; EC 2.6.1.1) is the prototype of the α-family enzymes (Alexander *et al.*, 1994), which are also named the 'AAT family' and have a type I fold. Type I fold enzymes were divided into subclasses based on the different structures of their N-terminal parts (Käck *et al.*, 1999). The crystal structure of *E. coli* cystathionine β-lyase (EC 4.4.1.8), the first representative of the γ-family, revealed that it belongs to the type I fold (Clausen *et al.*, 1996) and a structural subclass of enzymes belonging to the γ-family was named the cystathionine β-lyase subclass. The crystal structures of the MGLs from *P. putida* (PDB codes 1gco, 1ukj and 1pg8) and *T. vaginalis* (PDB codes 1e5f and 1e5e) demonstrate features characteristic of enzymes of the cystathionine β-lyase subclass.

The MGLs from *P. putida*, *T. vaginalis* and *C. freundii*, like other enzymes from the cystathionine β-lyase subclass, exist as homotetramers with a molecular weight of about 200 kDa that posses 222 symmetry. As in the case of many PLP-dependent enzymes of the AAT family, the tetrameric molecule of MGL can be subdivided into two so-called catalytic dimers in which the active sites contain residues from the other subunit (Fig. 2*a*, red/green and blue/yellow

subunits). Two catalytic dimers make up the tetrameric molecule of the enzyme.

Each subunit consists of three different domains: the N-terminal domain, the PLP-binding domain and the C-terminal domain (Figs. 2*b* and 2*c*).

The extended N-terminal domain (residues 1–63; Fig. 3) is composed of helices α1 and α2 which connect a long loop structure containing 25 residues. *C. freundii* MGL has a short 3_{10}-helix at the N-terminus in contrast to the unstructured N-termini of the MGLs from *P. putida* and *T. vaginalis*. The N-terminal domain protrudes from the PLP-binding domain of the subunit and provides most of the contacts to neighbouring subunits. In the catalytic dimer, residues of the α1 helix from one subunit (Fig. 2*a*, red) contact with the β12/α15 and β10/β11 loops of the C-terminal domain of the second subunit (Fig. 2*a*, green). Residues 28–34 make a β-strand structure paired with the same region of the subunit from the other catalytic dimer (Fig. 2*a*, blue), thus stabilizing the whole MGL tetramer by making a short antiparallel β-sheet (Fig. 1). Additional stabilization of the tetramer packing is provided by the contacts of the α2 helix and the preceding five residues with β11 and the adjacent short 3_{10}-helix of the C-terminal domain of another subunit of the neighbouring catalytic dimer (Fig. 2*a*, yellow).

The large PLP-binding domain (residues 64–259; Fig. 3) includes a seven-stranded mainly parallel β-sheet (β1–β7). Characteristically for PLP-dependent enzymes, it has directions +−+++++, with eight α-helices (3–10) and one 3_{10}-helix arranged on both sides of the β-sheet. Helices α3, α6, α7, α8, α10 and a short 3_{10}-helix adjacent to α8 are located on one side of the β-sheet and shield it from solvent. Helices α4, α5 and α9 are located on the other side of the β-sheet and are included in the intermolecular interface. PLP is covalently attached to Lys210 and is located near the N-terminus of helix α4 and the C-termini of strands β5, β6 and β7. There are no contacts between PLP and the C-terminal domain. The arrangement of the PLP-binding residues is almost identical in all known MGL structures (Fig. 4) and can be superimposed with root-mean-square deviations of 0.27 Å (*P. putida versus C. freundii*) and 0.19 Å (*T. vaginalis versus C. freundii*). The main discrepancies are in the region of the contacts between PLP and the N-terminal domain of the other subunit of a catalytic dimer. In *T. vaginalis* MGL two highly conservative residues (Tyr56 and Arg58) make contacts with the phosphate group of PLP, but in *C. freundii* MGL only the corresponding Arg60 makes a contact (Table 2), whereas Tyr58 is directed in the opposite direction.

The C-terminal domain (residues 260–398; Fig. 3) consists of a five-stranded β-sheet with five α-helixes (α11, α12, α13, α14, α15) located on the both sides of the β-sheet. Helices α11, α12, α13 and α15 continue the solvent shield of the α-helices layer of the PLP-binding domain. Helix α14 is in the PLP-binding/C-terminal interdomain interface, but no atoms of α14 make contacts with PLP-domain

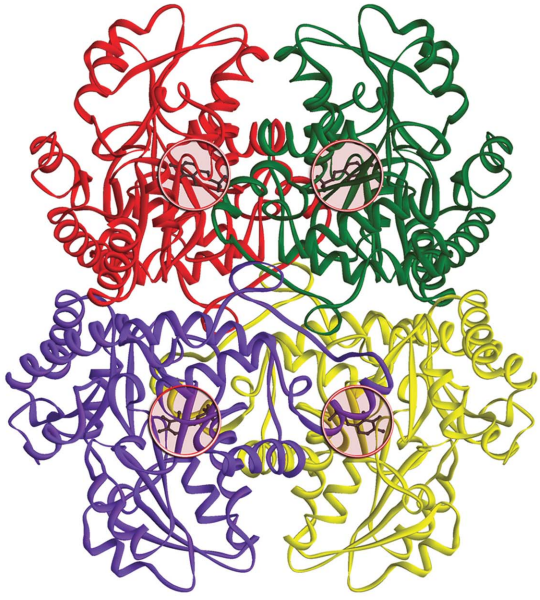

Figure 2
(*a*) Schematic model of MGL tetramer. Subunits are shown in different colours. PLP-binding sites are shown by pink circles. (*b*) Schematic representation of a monomer. The N-terminal domain is shown in magenta, the PLP-binding domain is in orange and the C-terminal domain is in blue. PLP is shown in ball-and-stick representation. (*c*) Topology diagram of a monomer.

Table 2
The distances between PLP and protein atoms in known MGL structures.

* represents residues from the other subunit of a catalytic dimer.

C. freundii MGL (PDB code 1y4i)			*T. vaginalis* MGL (PDB code 1e5f)			*P. putida* MGL (PDB code 1ukj)		
Residue	PLP atom	Distance (Å)	Residue	PLP atom	Distance (Å)	Residue	PLP atom	Distance (Å)
Tyr58* OH	O1P	–	Tyr56* OH	O1P	2.42	Tyr59* OH	O2P	2.45
Arg60* NE	O3P	–	Arg58* NE	O3P	2.59	Arg61* NE	O3P	3.08
Arg60* NH2	O2P	2.97	Arg58* NH2	O1P	2.93	Arg61* NH2	O2P	3.03
Gly88 N	O1P	2.71	Gly86 N	O2P	2.81	Gly89 N	O1P	2.82
Gly88 N	O3P	3.16	Gly86 N	O3P	3.10	Gly89 N	O3P	3.04
Ile89 N	O3P	2.92	Met87 N	O3P	2.87	Met90 N	O3P	2.80
Asp185 OD2	N1	2.73	Asp184 OD2	N1	2.64	Asp186 OD2	N1	2.70
Ser207 OG	O1P	2.82	Ser206 OG	O1P	2.81	Ser208 OG	O1P	3.05
Ser207 OG	O4P	2.92	Ser206 OG	O4P	2.92	Ser208 OG	O4P	2.77
Thr209 OG1	O1P	2.67	Thr208 OG1	O2P	2.78	Thr210 OG1	O1P	2.71

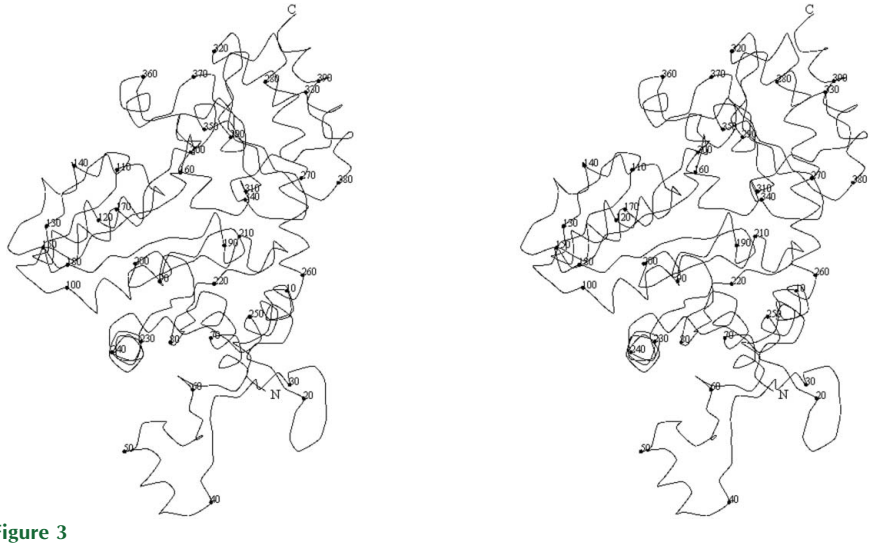

Figure 3
Stereoview of the C^{α} trace of a monomer. Every tenth C^{α} atom is represented by a sphere.

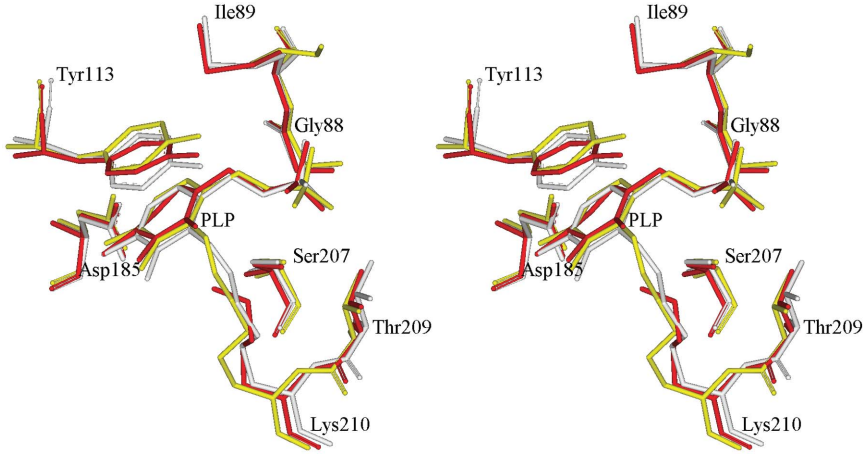

Figure 4
The superposition of the PLP-binding sites of *C. freundii* (yellow), *T. vaginalis* (red) and *P. putida* (grey) MGLs.

atoms. The position of this helix is different from that in *T. vaginalis* MGL, where α14 is located closer to the PLP-binding domain; it is located very close to the position of the corresponding helix in *P. putida* MGL.

We thank N. P. Fomenkova for excellent technical assistance. This work was supported by the Russian Academy of Sciences, the Russian Foundation for Basic Research (grant No. 05-04-48010), the Program of the RAS on Molecular and Cellular Biology and the Council of the RF President (grants for outstanding scientific schools Nos. 1969.2003.4 and 1800.2003.4). The research of AN was supported in part by the Russian Science Support Foundation. The research of MG was supported in part by an International Research Scholar's award from the Howard Hughes Medical Institute. Partial support for TVD was provided by the International Fogarty Foundation (grant No. 1 R03 TW006045-01A2)

References

Alexander, W., Sandmeir, E., Mehta, P. K. & Christen, P. (1994). *Eur. J. Biochem.* **219**, 953–960.
Brünger, A. T., Adams, P. D., Clore, G. M., DeLano, W. L., Gros, P., Grosse-Kunstleve, R. W., Jiang, J.-S., Kuszewski, J., Nilges, M., Pannu, N. S., Read, R. J., Rice, L. M., Simonson, T. & Warren, G. L. (1998). *Acta Cryst.* D**54**, 905–921.
Clausen, T., Huber, R., Laber, B., Pohlenz, H. D. & Messershmidt, A. (1996). *J. Mol. Biol.* **262**, 202–204.
Faleev, N. G., Troitskaya, M. V., Ivoilov, V. S., Karpova, V. V. & Belikov, V. M. (1994). *Prikl. Biokhim. Microbiol.* **30**, 458–463.
Grishin, N., Phillips, M. A. & Goldsmith, E. J. (1995). *Protein Sci.* **4**, 1291–1304.
Hoffman, R. M. (1997). *Hum. Cell*, **10**, 69–80.
Jansonius, J. N. (1998). *Curr. Opin. Struct. Biol.* **8**, 759–769.
John, R. A. (1995). *Biochim. Biophys. Acta*, **1248**, 81–96.
Jones, T. A., Zou, J. Y., Cavan, S. W. & Kjeldgaard, M. (1991). *Acta Cryst.* A**47**, 110–119.
Kabsch, W. (1993). *J. Appl. Cryst.* **26**, 795–800.
Käck, H., Sandmark, J., Gibson, K., Schneider, H. & Lindqvist, Y. (1999). *J. Mol. Biol.* **291**, 857–876.
Manukhov, I. V., Mamaeva, D. V., Rastorguev, S. M., Faleev, N. G., Morozova, E. A., Demidkina, T. V. & Zavilgelsky, G. B. (2005). In the press.
Motoshima, H., Imagaki, K., Kumasaka, T., Furuichi, T., Inoe, H., Tamura, T., Esaki, N., Soda, K., Tanaka, N., Yamamoto, M. & Tanaka, H. (2000). *J. Biochem.* **128**, 349–354.
Navaza, J. (1994). *Acta Cryst.* A**50**, 157–163.
Qu, K., Martin, D. L. & Lawrence, C. E. (1998). *Protein Sci.* **7**, 1092–1105.
Tanaka, H., Esaki, N. & Soda, K. (1977). *Biochemistry*, **16**, 100–106.
Tanaka, H., Esaki, N. & Soda, K. (1985). *Enzyme Microb. Technol.* **7**, 530–537.